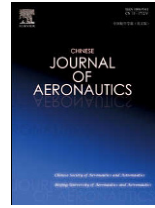




Contents lists available at ScienceDirect

# Chinese Journal of Aeronautics

journal homepage: [www.elsevier.com/locate/cja](http://www.elsevier.com/locate/cja)

## Safety Analysis of Flow Parameters in a Rotor-stator Cavity

ZHANG Gong<sup>a,b</sup>, DING Shuting<sup>a,b,\*</sup>

<sup>a</sup>*Airworthiness Technologies Research Center, Beihang University, Beijing 100191, China*

<sup>b</sup>*National Key Laboratory of Science and Technology on Aero-Engine Aero-thermodynamics, School of Jet Propulsion, Beihang University, Beijing 100191, China*

Received 12 August 2011; revised 9 September 2011; accepted 23 September 2011

### Abstract

In order to ensure the safety of engine life limited parts (ELLP) according to airworthiness regulations, a numerical approach integrating one-way fluid structure interaction (FSI) and probabilistic risk assessment (PRA) is developed, by which the variation of flow parameters in a rotor-stator cavity on the safety of gas turbine disks is investigated. The results indicate that the flow parameters affect the probability of fracture of a gas turbine disk since they can change the distribution of stress and temperature of the disk. The failure probability of the disk rises with increasing rotation Reynolds number and Chebyshev number, but descends with increasing inlet Reynolds number. In addition, a sampling based sensitivity analysis with finite difference method is conducted to determine the sensitivities of the safety with respect to the flow parameters. The sensitivity estimates show that the rotation Reynolds number is the dominant variable in safety analysis of a rotor-stator cavity among the flow parameters.

*Keywords:* airworthiness; aircraft engines; engine life limited parts; safety analysis; rotor-stator cavity; risk assessment

### 1. Introduction

The rotor-stator cavity is typical in the design of an aero-engine cooling system. It has significant influence on the safety of gas turbine disks which are engine life limited parts (ELLP) in compliance with the requirement of FAR33.70 since the fracture of a gas turbine disk could directly induce non-containment of high-energy debris, resulting in catastrophic events like loss of aircraft and human life<sup>[1-4]</sup>. Therefore, it is necessary to consider the rotor-stator cavity during the design and certification processes; otherwise it could cause fracture of turbine disks and hazardous engine effect.

A rotor-stator cavity is a cooling configuration in

which a disk rotates closely to a stationary casing where the air flow in the space between the disk and the casing is used as coolant. The traditional design of the rotor-stator cavity is rather complex, involving considerable iterations steps. The design process can be briefly described as follows: the first step is to design the structure of the cavity and determine geometrical parameters of the cavity such as the distance between the casing and the disk; then the fluid flow and heat transfer characteristics are calculated and verified with a fixed geometry of the cavity to investigate and determine flow parameters such as inlet Reynolds number  $Re$  and rotation Reynolds number  $Re_\omega$ ; the failure probability of the disk is predicted at the final step. These three steps are not repeated until the design satisfies the safety requirement of airworthiness. The process indicates that airworthiness compliance cannot be effectively judged during the design of the cavity. Moreover, it usually leads to several independent studies since the relationship of them is neglected in the sequence process. These studies can be simply separated into two categories: one is focused on the performance of the cavity; the other one is concentrated

\*Corresponding author. Tel.: +86-10-82338339.

E-mail address: [dst@buaa.edu.cn](mailto:dst@buaa.edu.cn)

Foundation item: Innovation Plan of Aero Engine Complex System Safety by the Ministry of Education Chang Jiang Scholars of China (IRT0905)

on the safety of the disk.

There are extensive investigations concerning fluid flow and heat transfer of rotor-stator systems<sup>[5-10]</sup>. Most of them examine the effect of parameters on cooling effectiveness or flow resistance by experimental verification or numerical simulation. Based on these previous studies, Owen pointed out that enhancing the cooling effectiveness and reducing the mass flow of coolant are important ways to improve turbine efficiency<sup>[11]</sup>. These prior studies play an important role in the design of the cavity. However, to date most investigations have been concerned with the effect of the cavity on engine performance, despite of the safety of the disk.

There are also many investigations regarding safety issue of aero-engines but none of them has focused on rotor-stator cavity by far. Meles, et al.<sup>[12]</sup> studied the turbine disk life and reliability based on finite element analysis and linear elastic fracture mechanism. They introduced the method of probabilistic analysis and discussed the effect of elements on the risk prediction. Leverant, et al.<sup>[13]</sup> introduced the design assessment of reliability with inspection (DARWIN) and its enhancement to assess the risk of rotating disks<sup>[14]</sup>. Aimed at enlarging the applicability of DARWIN, Enright, et al.<sup>[15-17]</sup> enhanced it in terms of various distributions of anomalies and random variables. In their investigation, DARWIN is used to assess the risk of disks of various geometries and materials. The sensitivity analysis results indicate that the effects of stress scatter, crack propagation rate scatter and initial flaw size distribution on the failure probability of the disk are different<sup>[18-19]</sup>. Based on the investigation of DARWIN's process details and data availability, Millwater<sup>[20]</sup> validated that DARWIN with the correct database is an acceptable means in compliance with the requirement of FAR33.70<sup>[4]</sup>. These investigations are all beneficial to the improvement of the safety of the disk. However, few attempts have been made with respect to the cavity though it is the crucial working environment of the disk.

Although many researches have been conducted to address fluid flow and heat transfer in the rotating cavity and the safety of disks, the effect of the cavity on the safety of the disk is rarely studied. This paper mainly focuses on the effect of flow parameters in the rotor-stator cavity with fixed geometry on the safety of the disk since the cavity geometry cannot be changed in the service of aero-engines. A numerical approach integrating fluid structure interaction (FSI) and probabilistic risk assessment (PRA) is established to investigate the variation of failure probability of the disk with respect to flow parameters in the cavity. A sensitivity analysis is also performed to identify the dominant variable in this field.

## 2. Methodology

Figure 1 shows the framework of the methodology we have established to perform the investigation. It

contains three essential steps. First, the variation of flow parameters of the rotating cavity is transferred to the loads of the disk by using one-way fluid structure interaction; then the loads, such as the temperature and stress distribution, are used as the input data of probabilistic risk assessment to predict the failure probability of the disk ( $P_f$ ); the sensitivity of  $P_f$  to the flow parameters is evaluated finally.

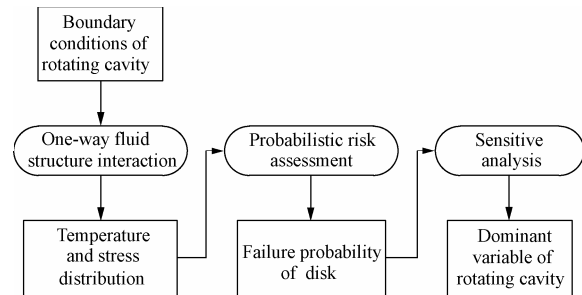


Fig. 1 Framework of methodology.

The analysis of rotor-stator cavity is conducted in fluid thermo-elasticity coupled field. The mathematical relation between the boundary conditions and the loads of the disk are expressed by high level nonlinear partial differential equations, which cannot be solved by using analytical approach in most conditions. The general way to solve such problems is employing non-dimensional algorithm, in which dimensionless parameters are defined. And then the effect of the dimensionless parameters on the cavity may be investigated by experimental work or numerical analysis.

Based on the non-dimensional analysis for the rotor-stator cavity of fixed geometry<sup>[3,5]</sup>, the temperature and stress distribution of the disk can be described as the functions of the dimensionless flow parameters

$$T = f(Re, Re_\omega, Te, Pr) \quad (1)$$

$$\sigma = h(Re, Re_\omega, Te, Pr) \quad (2)$$

where  $Re$  is the inlet Reynolds number,  $Re_\omega$  the rotation Reynolds number,  $Te$  the Chebyshev number and  $Pr$  the Prandtl number. Since  $Pr$  is almost invariant in the rotor-stator cavity, its effect on the stress and temperature distribution of the disk is usually ignored. And the other three flow parameters are formulated by

$$Re = \rho_0 v R_0 / \mu_0 \quad (3)$$

$$Re_\omega = \rho_0 \omega R_0 / \mu_0 \quad (4)$$

$$Te = \dot{q} R_0 / (\lambda_s T_0) \quad (5)$$

where  $\rho_0$  is the density of the cooling air at reference temperature,  $v$  the inlet velocity of the cooling air,  $R_0$  the radius of the disk which is considered as the reference length of the system,  $\mu_0$  the dynamic viscosity of the cooling air,  $\omega$  the rotational speed of the disk,  $\lambda_s$  the conductivity of the disk material,  $T_0$  the temperature of the cooling air, and  $\dot{q}$  the heat flux at the outer rim of the disk which is less than the maximum permissible heat flux;  $Re$ ,  $Re_\omega$  and  $Te$  represent the mass flow of the cooling air, the rotational speed of the disk and the heat

flux on the outer rim of the disk, respectively.

From Eqs. (1)-(5), it can be found that the dimensionless flow parameters,  $Re$ ,  $Re_\omega$  and  $Te$ , are independent variables governing the fluid flow, heat transfer and structure deformation in the rotating cavity. Hence to investigate the effect of the flow parameters on the load of the disk through multi-physical coupling, a numerical approach is adopted in this study.

Fluid structure interaction simulation is an effective numerical tool for multi-physical problems where the interaction between fluid analysis and structural analysis is taken into account. One-way fluid structure interaction, ignoring the effect of the structural deformation on the flow field, is adopted because the deformation of the structure can be neglected in this study. The simulation is performed by coupling solver packages including ANSYS CFX 11.0 and ANSYS Multiphysics 11.0. It calculates the loads of the disk much faster than two-way fluid structure interaction, in which the structural deformation is considered as an additional load in fluid analysis.

The input data of probabilistic risk assessment to predict  $P_f$  are the loads of the disk obtained from fluid structure interaction simulation. In order to calculate  $P_f$ , a computational package is developed based on the framework of probabilistic risk assessment shown in Fig. 2. The disk can be divided into some zones. The total risk for the disk is the probability union of the zones:

$$P_f = P[F_1 \cup F_2 \cup \dots \cup F_n] \quad (6)$$

where  $F_i$  represents the failure of zone  $i$ . The risk  $p_i$  in each zone can be described as the product of the conditional fracture probability  $p_{i|c}$  and the crack occurrence rate  $\lambda_i$ . Equation (6) may be reduced by [15]:

$$P_f \approx \sum_{i=1}^n p_i = \sum_{i=1}^n p_{i|c} \lambda_i \quad (7)$$

For a zone with an initial crack subject to simple loadings, the crack length  $a$  and stress intensity factor (SIF)  $K$  increase with increasing load cycles  $N$ . Failure occurs when the maximum  $K$  equals or exceeds the fracture toughness  $K_c$ :

$$g = K_c(T) - K(X, N) \leq 0 \quad (8)$$

where  $g$  is the fatigue life limit function. It is deduced from Eq. (8) that  $g$  is dependent on the number of load cycles  $N$ , temperature distribution  $T$  and variable  $X$  which is a function with respect to stress and crack length. A negative  $g$  indicates that a failure occurs. The failure probability of the zone  $i$  is

$$p_{i|c} = P[g(X, T, N) \leq 0] \quad (9)$$

The fracture toughness  $K_c$  is a function of temperature and it is obtained by interpolation of the available material property data based on the temperature distribution of the disk.  $K$  is a function with respect to crack length, crack geometry and loads.

$$K = G\sigma\sqrt{\pi a} \quad (10)$$

where  $\sigma$  is the stress of the crack area and  $G$  geometrical correction coefficient. The coefficient is derived

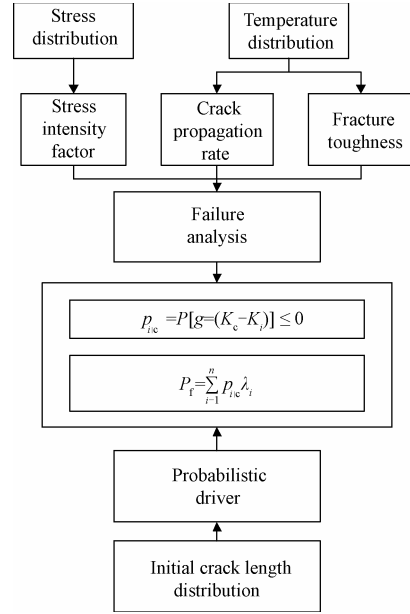


Fig. 2 Framework of probabilistic risk assessment.

from Newman's method in this study [21]. The crack length propagation is governed by Paris' Law:

$$\frac{da}{dN} = C(\Delta K)^n \quad (11)$$

where  $C$  and  $n$  are constant and index of the Paris' Law and associated with temperature distributions. Variable  $\Delta K$  denotes the maximal change of  $K$  and it can be calculated by the current crack length and the load of disk obtained from fluid structure interaction simulation. In this study, Eq. (11) is solved by using the Runge-Kutta method.

It can be derived from Eqs. (9)-(11) that

$$p_{i|c} = \int_{K_c(T)}^{K_{max}} G\sigma\sqrt{\pi} \int_0^{N_c} \frac{f(a)da}{dN} dN dK \quad (12)$$

where  $N_c$  is the number of current load cycles and  $f(a)$  the probability density function of initial crack length. Thus the risk of each zone is a function with respect to initial crack length, the stress distribution, the temperature distribution and the load cycles. Equations (1)-(2), Eq. (7) and Eq. (12) establish the relation between the crack length and the three flow parameters  $Re$ ,  $Re_\omega$  and  $Te$ .

Finally,  $P_f$  is calculated by the Monte Carlo method. The initiation crack length is chosen as the only random variable of the probabilistic driver in Monte Carlo simulation [22]. It is a probable way to predict  $P_f$  and has been provided in Advisory Circular 33.14-1 [1] and Advisory Circular 33.70-1 [2] as an acceptable means of compliance.

The probabilistic risk assessment approach may be verified by using calibration test case data provided in Advisory Circular 33.14-1 [1]. The calculation result without any inspection, based on the probabilistic risk assessment approach, is  $1.45 \times 10^{-9}$ . It is in the range of  $1.27 \times 10^{-9}$  -  $1.93 \times 10^{-9}$  acceptable in Advisory Cir-

cular [1]. Thus this probabilistic risk assessment approach is effective to predict the risk of engine life limited parts.

The sensitivity analysis is performed to identify the dominant variable of the rotor-stator cavity. The probabilistic sensitivity is defined as the partial derivative of  $P_f$  with respect to the flow parameters in the cavity. The non-dimensional sensitivity is also evaluated. It is a sampling based sensitivity of  $P_f$  estimate with finite difference method in this study. The finite difference estimates are obtained by perturbing the interested parameters and approximated by

$$S_\theta = \frac{\partial P_f}{\partial \theta} \approx \frac{\Delta P_f}{\Delta V_s} = \frac{P_f(\theta + \Delta\theta) - P_f(\theta - \Delta\theta)}{2\Delta V_s} \quad (13)$$

where  $P_f$  is the failure probability of the disk,  $S_\theta$  the sensitivity of  $P_f$  towards the flow parameter,  $\theta$  one interest flow parameter,  $\Delta\theta$  the perturbed flow parameter, and  $V_s$  the perturbation size. The perturbation size is chosen as 1% of flow parameters at nominal condition. A separate analysis must be performed for the sensitivity estimate of each flow parameter at the same perturbation size to determine the sensitivity of  $P_f$ .

### 3. Numerical Analysis

Present parametric study is carried out to investigate the influence of  $Re$ ,  $Re_\omega$  and  $Te$  on the safety of the disk by calculating  $P_f$  and identifying the dominant variable. The essential details for the numerical simulation such as model and boundary conditions are introduced and discussed in this section.

#### 3.1. Geometry and mesh

Because the disk is assumed axisymmetric, as shown in Fig. 3, the overall computational domain comprises only a sector of  $1^\circ$  angle with a periodic boundary condition specified on each side. The rotor-stator cavity model is meshed by hexahedron element to optimize for fluid structure interaction, as shown in Fig. 4. The domain consists of a stationary fluid part and a rotary solid part which is assumed as only half of the meridian plane since the model is symmetric. The radii of the outer and inner rims are 320 mm and 40 mm, respectively. The radius of coolant inflow, which is assumed

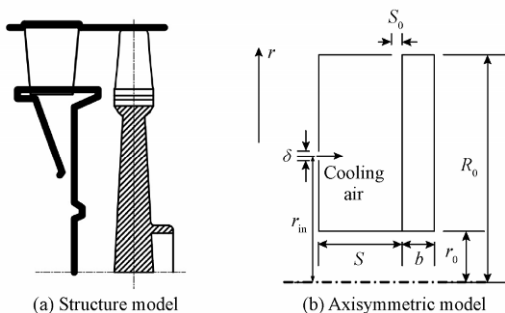


Fig. 3 Typical rotor-stator cavity structure and its axisymmetric model.

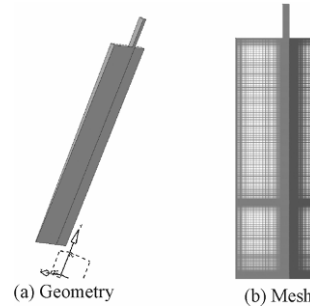


Fig. 4 Simulation model of rotor-stator cavity.

as seam instead of hole, is 128 mm with the length of 2.1 mm. The outflow section is extended 40 mm away from the outer rim to avoid the over flow in the boundary. The details of the cavity geometry are listed in Table 1. The number of the mesh is totally 81 150 and it has been validated that the effect of meshing density on the results is negligible.

Table 1 Geometry parameter of simulation model mm

$R_0$	$r_0$	$b$	$S$	$S_0$	$r_{in}$	$\delta$
320	40	30	64	8	128	2.1

#### 3.2. Boundary conditions and material properties

The numerical method used in fluid structure interaction is a finite volume, incompressible and steady solver. It employs a  $k-\Omega$  turbulence model which has been validated successfully to compute the fluid flow and heat transfer in a rotor-stator system. The effectiveness of the fluid structure interaction method is validated by experimental data [3] obtained at low rotation speeds of the cavity. Though lack of data at high rotation speeds, this method may also be available at such conditions since the flow Mach number in almost all the region of the cavity at high speed is still lower than 0.3. The materials of fluid and solid are assumed isotropic and homogeneous. The material properties are listed in Table 2. The crack propagation rate and  $K_{Ic}$  variation subject to different temperature are listed in Table 3.

Table 2 Material properties

Domain	Material property	Value
Fluid	Density $\rho / (\text{kg} \cdot \text{m}^{-3})$	1.173
	Thermal conductivity $\lambda_f / (\text{W} \cdot \text{m}^{-1} \cdot \text{K}^{-1})$	0.026 5
	Specific heat $c_p / (\text{J} \cdot \text{kg}^{-1} \cdot \text{K}^{-1})$	1 005
	Dynamic viscosity $\mu / (10^{-5} \text{ kg} \cdot \text{m}^{-1} \cdot \text{s}^{-1})$	1.854
Solid	Density $\rho / (\text{kg} \cdot \text{m}^{-3})$	8 240
	Thermal conductivity $\lambda_s / (\text{W} \cdot \text{m}^{-1} \cdot \text{K}^{-1})$	22
	Specific heat $c_p / (\text{J} \cdot \text{kg}^{-1} \cdot \text{K}^{-1})$	635
	Young's modulus $E / (10^9 \text{ Pa})$	203
	Poisson's ratio $\nu$	0.3
	Coefficient of thermal expansion $\alpha / (10^{-6} \text{ K}^{-1})$	14.6

**Table 3 Crack propagation rate and fracture toughness**

Temperature <i>T</i> /°C	Paris constant <i>C</i>	Paris index <i>n</i>	Fracture toughness <i>K<sub>c</sub></i> /(MPa·m <sup>1/2</sup> )
20	9.08×10 <sup>-13</sup>	5.19	103.5
300			89.0
500	7.04×10 <sup>-12</sup>	4.86	87.0
600	2.15×10 <sup>-10</sup>	3.98	83.0
650			69.5

Boundary conditions of this simulation include the mass flow rate of the cooling air, the rotation speed of the disk and the heat flux on the outer rim of the disk, etc. The mass flow rate of inlet cooling air varies from 400 kg/h to 1 200 kg/h with an increment of 100 kg/h. The rotational speed of the disk varies from 9 000 r/min to 10 000 r/min with an increment of 100 r/min. The heat flux on the outer rim of the disk varies from 15 000 W/m<sup>2</sup> to 25 000 W/m<sup>2</sup> with an increment of 1 000 W/m<sup>2</sup>. The external load is about 50 MPa, which is applied to the outer rim to simulate blade loading. The maximum principle stress is hoop stress. It is assumed that the crack grows under constant amplitude cyclic loadings until it is fractured. The interface between fluid phase and solid phase is modeled in the computational domain, which can be calculated by fluid structure interaction. Other details of boundary conditions are listed in Table 4. More than six million samples are used in Monte Carlo simulations, intended to obtain highly accurate result. Figure 5 shows the exceedance curve representing a function of initiation crack size distribution, which is obtained from industry defined data [1]. In Fig. 5, 1 mils = 0.025 4 mm. The aspect ratio of the initial crack is assumed to be 1.

**Table 4 Boundary conditions for the simulation**

Boundary type	Boundary conditions detail
Temperature of inlet coolant /K	780
Pre-swirl angle of inlet coolant /(°)	0
Outlet pressure/Pa	101 325
The wall of stationary casing	No slip, adiabatic
The leeward of the disk	No axis displacement, adiabatic

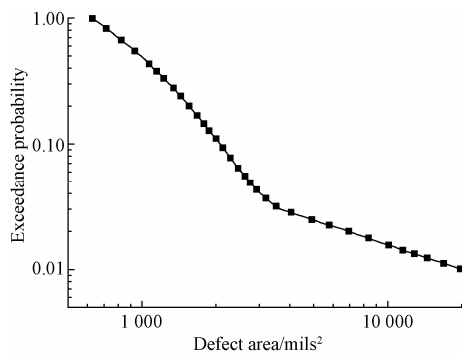


Fig. 5 Initial crack size distribution.

**4. Results and Discussion**

**4.1. Effects of flow parameters**

The numerical results are shown in Figs. 6-9. Figure 6 illustrates the typical failure probability of the disk as a function of load cycles.  $P_f$  of the disk subject to nominal condition is  $1.33 \times 10^{-11}$ , which means that  $Re$  is  $1.28 \times 10^6$ ,  $Re_\omega$  is  $6.45 \times 10^6$  and  $Te$  is 0.37.  $P_f$  is much less than  $10^{-8}$  and therefore it meets the safety requirement of the airworthiness regulations since the load of the disk at the simulation conditions is less severe than the real operating conditions of aero-engines.

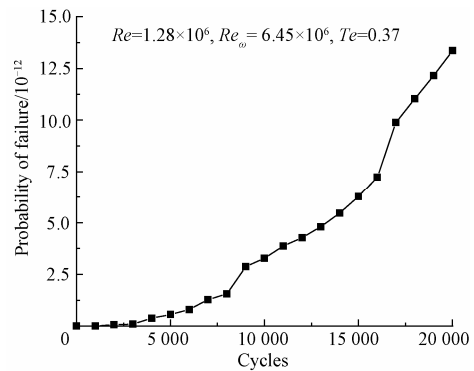


Fig. 6 Failure probability of the disk.

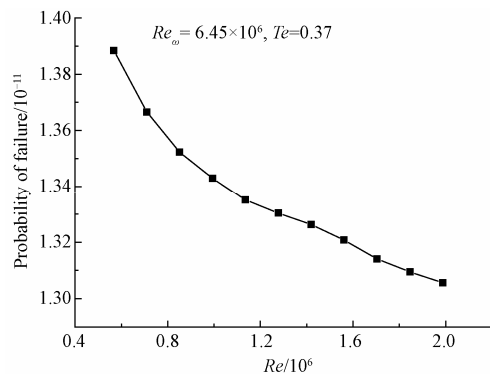


Fig. 7 Failure probability with increasing  $Re$ .

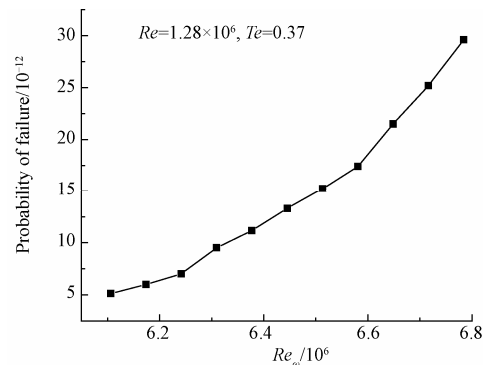


Fig. 8 Failure probability with increasing  $Re_\omega$ .

$P_f$  at 20 000 cycles decreases from  $1.39 \times 10^{-11}$  to  $1.31 \times 10^{-11}$  with  $Re$  rising from  $5.68 \times 10^5$  to  $1.99 \times 10^6$ ,

as illustrated in Fig. 7. It decreases rapidly at low  $Re$  but slowly at high  $Re$ . It is observed that the trend with  $Re$  is different from the trend with  $Re_\omega$  or  $Te$ .  $P_f$  increases from  $5.13 \times 10^{-12}$  to  $2.96 \times 10^{-11}$  with  $Re_\omega$  increasing from  $6.11 \times 10^6$  to  $6.78 \times 10^6$ , and increases from  $1.24 \times 10^{-11}$  to  $1.40 \times 10^{-11}$  with  $Te$  increasing from 0.28 to 0.47 (see Figs. 8-9). The increasing rate of  $P_f$  is also different with the variations of  $Re_\omega$  and  $Te$ .

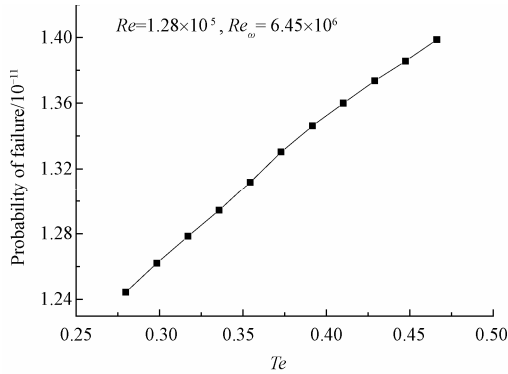


Fig. 9 Failure probability with increasing  $Te$ .

Resulting from fluid structure interaction simulations, the relations between maximum hoop stress, temperature and different flow parameters are derived and illustrated in Figs. 10-11 respectively. It is found that the flow parameters do influence  $P_f$  because they can change the distribution of temperature and stress of the disk. The stress can affect the stress intensity factor of the crack and the elevated temperature can affect the crack propagation rate and fracture toughness of the material as shown in Table 3. The stress decreases with increasing  $Re$ , as shown in Fig. 10, whereas the elevated temperature decreases rapidly at low  $Re$  but slowly at high  $Re$ . The reduction of either temperature or stress benefits the improvement of the safety of the disk, thus  $P_f$  decreases with the variation of  $Re$ , as was mentioned above. The effect of  $Re_\omega$  on  $P_f$  is different. The elevated temperature is almost unchanged but the hoop stress changes largely when  $Re_\omega$  increases.  $P_f$  increases with the great increase of stress level and relatively constant temperature, which means consistent crack propagation rate and fracture toughness but large SIF of the initial crack. The results show a re-

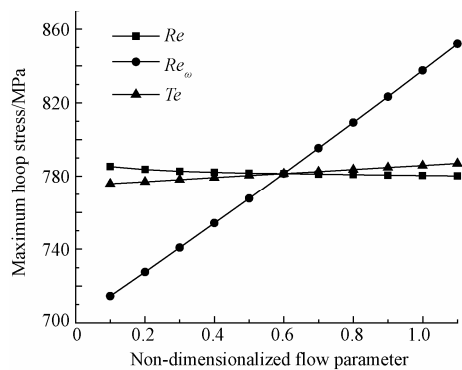


Fig. 10 Maximum hoop stress of the disk.

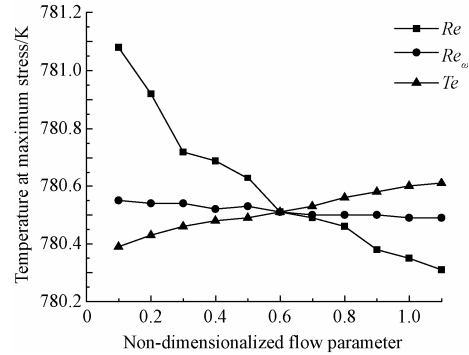


Fig. 11 Temperature at the location with maximum stress.

verse trend of the variation of the elevated temperature and stress with the increase of  $Te$  compared to that with  $Re$ . The increase of the flux on the outer rim of the disk causes the rise of temperature level, as well as the stress level. Hence  $P_f$  increases with increasing  $Te$ , as illustrated in Fig. 9. The results indicate that the effect of the parameters on the safety of disk is rather complex.

#### 4.2. Sensitivity analysis

The direct sensitivity of  $P_f$  with respect to the flow parameters is obtained from the results of probabilistic risk assessment as shown in Table 5. A positive sensitivity indicates that an increase in the flow parameter will increase  $P_f$ , and conversely, a negative sensitivity indicates that an increase in the flow parameter will decrease  $P_f$ .  $S_{Re}$  ( $S_{Re}$  represents the sensitivity of  $P_f$  to  $Re$ ) is  $-3.84 \times 10^{-19}$  when  $Re$  is  $5.68 \times 10^5$ , which means a unit augment of  $Re$  leads to the decrease of  $P_f$  by  $3.84 \times 10^{-19}$ , and drops to  $-1.95 \times 10^{-20}$  when  $Re$  is  $1.99 \times 10^6$ . The magnitude of sensitivity is relatively small because the variation of  $Re$  is usually at the order of  $10^5$  or  $10^6$ . The sensitivity declines because the flow structure changes with increasing  $Re$ . In addition, the temperature gradient at the inner rim reduces with increasing  $Re$ . The thermal stress decreases significantly at low  $Re$  but slowly at high  $Re$  when centrifugal stresses are constant, so the total hoop stress declines obviously at low  $Re$ . The results indicate that  $S_{Te}$  ( $S_{Te}$  represents the sensitivity of  $P_f$  to  $Te$ ) is larger than  $S_{Re}$  and  $S_{Re_\omega}$  ( $S_{Re_\omega}$  represents the sensitivity of  $P_f$  to  $Re_\omega$ ), thus  $Te$  seems to be the dominant variable among

Table 5 Sensitivity estimates

Flow parameter	Value	Sensitivity of $P_f$
$Re$	$5.68 \times 10^5$	$-3.84 \times 10^{-19}$
	$1.28 \times 10^6$	$-3.21 \times 10^{-20}$
	$1.99 \times 10^6$	$-1.95 \times 10^{-20}$
$Re_\omega$	$6.11 \times 10^6$	$1.40 \times 10^{-19}$
	$6.45 \times 10^6$	$2.97 \times 10^{-19}$
	$6.78 \times 10^6$	$6.53 \times 10^{-19}$
$Te$	0.28	$6.32 \times 10^{-13}$
	0.37	$4.23 \times 10^{-13}$
	0.47	$2.79 \times 10^{-13}$

the flow parameters in the rotating cavity. The results are confusing since the magnitude of  $Te$  is much less than that of  $Re$  and  $Re_\omega$ . Hence it is necessary to identify the dominant variable by non-dimensional sensitivity estimates.

The non-dimensional sensitivity of  $P_f$  with regard to the perturbed flow parameters at the nominal condition is shown in Fig. 12. The perturbation magnitude is chosen as 1% of flow parameters at the nominal condition. The results indicate that the dominate variable in the rotor-stator cavity is  $Re_\omega$ , followed by  $Te$  and  $Re$ . The results of non-dimensional sensitivity analysis reveal that the sensitivity of  $P_f$  to  $Re_\omega$  is  $3.68 \times 10^{-12}$  which is about 27% of  $P_f$  at the nominal condition. Therefore, the effect of the flow parameters in the rotor-stator cavity is significant and needs careful consideration in the design and certification process.

It is illustrated in Fig. 12 that the effects of  $Te$  and  $Re$  on  $P_f$  are negligible to structures of high rotational speed and large radius when the three parameters vary at the same order. This is a consequence associated with the variation of centrifugal stress induced by different values of  $Re_\omega$  since the effect of centrifugal stress on  $P_f$  is more significant than other factors like temperature or thermal stress, under the conditions given in the present study. It should be noticed that this conclusion is applicable to rotors under general operation conditions of aero-engine, while it may not be suitable to those rotational structures under other working conditions.

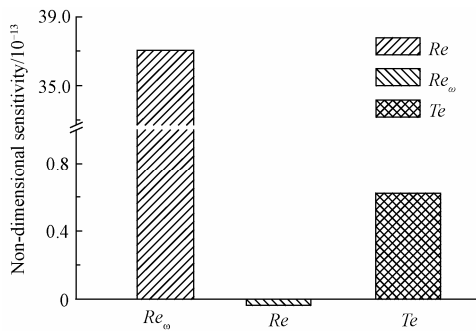


Fig. 12 Non-dimensional sensitivity of flow parameters.

## 5. Conclusions

1) A numerical framework of safety analysis of the rotor-stator cavity is established by integrating one-way fluid structure interaction and probabilistic risk assessment method. One-way fluid structure interaction using coupled solver packages ANSYS CFX 11.0 and ANSYS Multiphysics 11.0 is implemented to calculate the loads of the disk as the input data of probabilistic risk assessment. A computational package, consisting of SIF calculator, Paris equation solver and Monte Carlo simulator, is also developed to predict the risk of the disk failure.

2) The numerical results show that the variation of flow parameters in the rotor-stator cavity can influence

$P_f$ . The effects of  $Re$ ,  $Re_\omega$  and  $Te$  on  $P_f$  are different because their impacts on the stresses and the temperature distributions of the disk are different.  $P_f$  increases with increasing  $Re_\omega$  and  $Te$ , but decreases with increasing  $Re$ .

3) The results of the sensitivity analysis reveal that  $Re_\omega$  is the dominant variable to estimate the risk of the rotor-stator cavity since the variation of  $Re_\omega$  can affect the stress level significantly while the variations of  $Re$  and  $Te$  have less effect than the former one.

## Acknowledgments

We would like to thank the reviewers for their constructive and insightful suggestions for further improving the quality of this paper and to express our profound gratitude to Prof. John Holmes and Dr. Qiang Pan for revising the paper writing.

## References

- [1] Advisory Circular 33.14-1. Damage tolerance for high energy turbine engine rotors. Washington D.C.: FAA, 2001.
- [2] Advisory Circular 33.70-1. Guidance material for aircraft engine-life-limited parts requirements. Washington D.C.: FAA, 2009.
- [3] Fu D B, Tao Z, Zhang G, et al. Safety evaluation of cooling configuration in a rotor-stator cavity. Proceedings of 2009 International Symposium on Aircraft Airworthiness, 2009; 376-381.
- [4] CFR 14 part 33. Airworthiness standards: aircraft engines. Washington D.C.: FAA, 2009.
- [5] Ong C L, Owen J M. Prediction of heat transfer in a rotating cavity with a radial outflow. Journal of Turbomachinery 1991; 113(1): 115-122.
- [6] Iacovides H, Chew J W. The computation of convective heat transfer in rotating cavities. International Journal of Heat and Fluid Flow 1993; 14(2): 146-154.
- [7] Farthing P R, Long C A, Owen J M, et al. Rotating cavity with axial throughflow of cooling air: heat transfer. Journal of Turbomachinery 1992; 114(1): 229-236.
- [8] Farthing P R, Long C A, Owen J M, et al. Rotating cavity with axial throughflow of cooling air: flow structure. Journal of Turbomachinery 1992; 114(1): 237-246.
- [9] Karabay H, Pilbrow R, Wilson M, et al. Performance of pre-swirl rotating-disc systems. Journal of Engineering for Gas Turbines and Power 2000; 122(3): 442-450.
- [10] Karabay H, Wilson M, Owen J M. Predictions of effect of swirl on flow and heat transfer in a rotating cavity. International Journal of Heat and Fluid Flow 2001; 22(2): 143-155.
- [11] Owen J M. Modelling internal air systems in gas turbine engines. Journal of Aerospace Power 2007; 22(4): 505-520. [in Chinese]
- [12] Melis M E, Zaretsky E V, August R. Probabilistic analysis of aircraft gas turbine disk life and reliability. Journal of Propulsion and Power 1999; 15(5): 658-666.
- [13] Leverant G R, Littlefield D L, McClung R C, et al. A probabilistic approach to aircraft turbine rotor material design. ASME Paper, 1997-GT-22, 1997.
- [14] Leverant G R, Millwater H R, McClung R C, et al. A new tool for design and certification of aircraft turbine

- rotors. *Journal of Engineering for Gas Turbines and Power* 2004; 126(1): 155-159.
- [15] Enright M P, McClung R C, Huyse L. A probabilistic framework for risk prediction of gas turbine engine components with inherent or induced material anomalies. ASME Paper, 2005-GT-68982, 2005.
- [16] Enright M P, Huyse L, McClung R C. Fracture mechanics-based probabilistic life prediction of components with large numbers of inherent material anomalies. 9th International Conference on Structural Safety and reliability, 2005; 601-607.
- [17] Enright M P, Huyse L. Methodology for probabilistic life prediction of multiple-anomaly materials. *AIAA Journal* 2006; 44(4): 787-793.
- [18] Millwater H R, Osborn R W. Probabilistic sensitivities for fatigue analysis of turbine engine disks. *International Journal of Rotating Machinery* 2006; 2006: 1-12.
- [19] Enright M P, Wu Y T. Probabilistic fatigue life sensitivity analysis of titanium rotors. AIAA-2000-1647, 2000.
- [20] Millwater H R, Enright M P, Fitch S H K. A convergent probabilistic technique for risk assessment of gas turbine disks subject to metallurgical defects. AIAA-2002-1382, 2002.
- [21] Newman J C, Raju I S. Stress-intensity factor for cracks in three-dimensional finite bodies. NASA TM 83200, 1981.
- [22] Advisory Circular 33.70-2. Damage tolerance of hole features in high-energy turbine engine rotors. Washington D.C.: FAA, 2009.

### Biographies:

**ZHANG Gong** received B.S. degree at Beihang University in 2006, and then became a Ph.D. student there. His main research interests are airworthiness design technologies of aero-engines and safety analysis of engine life limited parts.  
E-mail: zhanggong@sjp.buaa.edu.cn

**DING Shuiting** is a professor and Ph.D. supervisor at School of Jet Propulsion, Beihang University, Beijing, China. He received the Ph.D. degree from the same university in 1998. His current research interests are airworthiness technologies and aero-engine design.  
E-mail: dst@buaa.edu.cn